

Capacitive-Resistive Measurements of Cobalt-Phthalocyanine Organic Humidity Sensors

Mohammed T. HUSSEIN*, Iqbal S. NAJI, Ameer F. ABDULAMEER,
Eman K. HASSEN, and Muataz S. BADRI

Department of Physics, College of Science, University of Baghdad, Baghdad, Iraq

*Corresponding author: Mohammed T. HUSSEIN E-mail: odayhammadi@rocketmail.com

Abstract: In this study, the fabrication and characterization of capacitive humidity sensors using cobalt-phthalocyanine (CoPc) as the active material were presented. Thin films of CoPc were deposited by drop casting on glass substrates with pre-deposited aluminum electrodes to form Al/CoPc/Al surface-type humidity sensors. The effect of humidity on the electrical properties of the CoPc film was investigated by measuring capacitance and resistance of the samples at four different frequencies of the applied voltage. It was observed that the capacitance of the sensor increased while the resistance decreased with raising the relative humidity. It was also found that the values of capacitance and resistance decreased with increasing frequency. The optical absorption spectra and optical band gap energy of CoPc films were measured. The structure of CoPc powder and thin films has been studied by X-ray diffraction (XRD), scanning electron microscopy (SEM), and atomic force microscopy (AFM). Results of XRD studies show that the film structure is polycrystalline with the monoclinic structure while thin films have a peak for annealing temperatures with (100) orientation. Also, the surface morphology (grain size and roughness) for CoPc films have been studied by AFM.

Keywords: Organic humidity sensors, CoPc, capacitance, resistance

Citation: Mohammed T. HUSSEIN, Iqbal S. NAJI, Ameer F. ABDULAMEER, Eman K. HASSEN, and Muataz S. BADRI, "Capacitive-Resistive Measurements of Cobalt-Phthalocyanine Organic Humidity Sensors," *Photonic Sensors*, 2015, 5(3): 257–262.

1. Introduction

Humidity sensors are important for the assessment of environmental monitoring and industrial applications [1–3]. Humidity sensors have several categories based on their measuring principles, which include capacitive, resistive, hygrometric, gravimetric, optical, and integrated types [4–6]. Organic-based humidity sensors are divided into two types: resistive and capacitive [7]. The capacitive-type humidity sensors show good linearity and exhibit better stability at higher

humidity levels as compared to resistive humidity sensors.

The characterization of organic semiconductors is receiving great attention because of the increased activity in their synthesis and potential use in a wide range of large area flexible, disposable, electric, electronic, and photonic devices, such as rechargeable batteries, junction diodes [8], organic field effect transistor (OFET) [9], memory, solar cells [10], organic light emitting diodes (OLEDs) [11], and sensors [12]. Therefore, the investigation into the properties of the organic semiconductor

Received: 21 April 2015 / Revised version: 10 June 2015

© The Author(s) 2015. This article is published with open access at Springerlink.com

DOI: 10.1007/s13320-015-0257-9

Article type: Regular

under different conditions is a very promising field for the development of various sensors. Humidity is one of the most common constituents present in the environment. Therefore, humidity sensors are required for the measurement and control of humidity in many fields, such as industrial production, human comfort, medicine and agriculture, food storage and medicine stores [13, 14]. CoPc, whose chemical formula is $C_{32}H_{16}CoN_8$, is an organic semiconductor with excellent chemical stability against heat, light, moisture and oxygen, low heat conduction, and diversity of optical properties.

In this paper, the fabrication and investigation of Al/CoPc/Al surface-type capacitive humidity sensors and the effect of humidity on the capacitance are studied. The optical band gap of CoPc thin films is also studied.

2. Experiment

Figure 1 shows the molecular structure of CoPc used as an active material. The glass substrate was thoroughly cleaned in deionized water using an ultrasonic bath for 10 minutes and dried for 5 minutes. Aluminum electrodes of 100 nm thickness were deposited by means of a thermal evaporation technique on a cleaned glass substrate using a proper desired mask. All electrodes were deposited at a deposition rate of 0.1 nm/s, and the pressure remains constant at 10^{-5} mbar during thermal deposition. The gap between electrodes and length of the gap were equal to 40 μm and 25 mm, respectively. An amount of 10 mg CoPc powder (0.9999 pure, Sigma-Aldrich) dissolved in 1 ml of dimethyl sulfoxide (DMSO) was mixed for one hour at room temperature and drop-casted on glass substrates with pre-deposited surface-type metallic electrodes to construct Al/CoPc/Al samples, which were dried for 2 hours at the temperature of 155 $^{\circ}\text{C}$ to fabricate the final Al/CoPc/Al humidity sensors. The structure of the fabricated sensors is shown in Fig. 2. The effect of humidity on the electrical properties of the fabricated sensors was investigated by measuring

the capacitance and resistance of the samples at four different frequencies of the applied voltage: 12 Hz, 100 Hz, 300 Hz, and 600 Hz. The optical properties and the band gap were also measured.

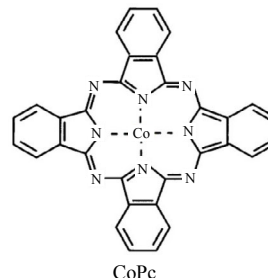


Fig. 1 Molecular structure of cobalt phthalocyanine (CoPc).

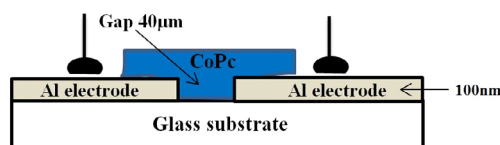


Fig. 2 Schematic cross-section view of the Al/CoPc/Al structure.

3. Results and discussion

The XRD spectrum of CoPc film sample exhibits the polycrystalline structure with monoclinic phase, while the XRD spectrum of the CoPc powder, shown in Fig. 3, exhibits sharp peaks at reflection surfaces of (100), ($\bar{1}02$), ($\bar{2}02$), and ($\bar{1}04$) and lower intensities for other peaks.

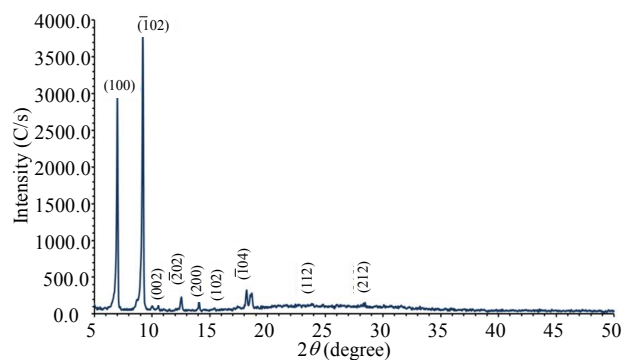


Fig. 3 XRD spectrum of CoPc powder.

The XRD patterns of CoPc thin films at two different temperatures were recorded, and the structural parameters were calculated as shown in Fig. 4. These patterns display strong reflections at (100) orientation, and we can observe that the

reflection from other planes has disappeared. The XRD pattern has shown a high peak at (100) plane at the temperature of 298K, and the intensity of (100) plane has increased at the temperature of 428 K, which means better arrangement and more crystallinity. This also means that the crystallization of the film is a function of the annealing temperature, and this result is agreed with the previous study [15]. The grain size of the crystallites was calculated from the XRD results using Scherrer’s relation to increase from 17.7 nm at the room temperature of 298 K to 28.4 nm at the annealing temperature of 428 K.

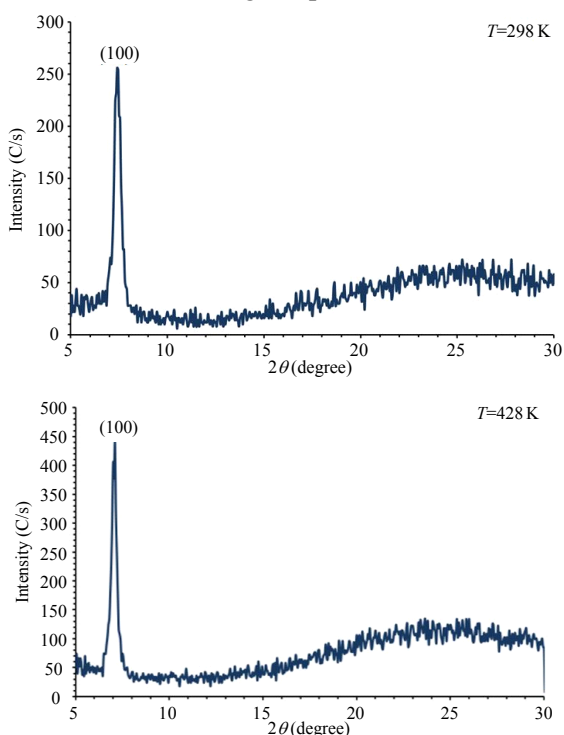


Fig. 4 XRD patterns of CoPc thin films prepared at different annealing temperatures (298 K and 428 K).

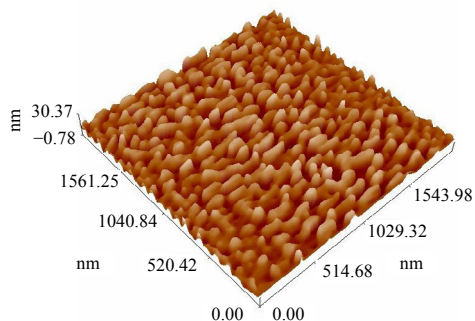


Fig. 5 3D AFM image of the CoPc thin film prepared at annealing temperature of 428 K.

Surface morphology of the CoPc film (see Fig. 5)

shows that the morphology has a large number of grain size, which indicates the crystalline nature of the film because it was prepared at the temperature higher than the room temperature. Due to heating effect, grain growth will take place and result in the crystallinity and good surface morphology [16–18].

The scanning electron microscopy (SEM) images of the thin film CoPc samples prepared by drop-casting and dried at the temperature of 428 K for 2 hours are shown in Fig. 6(a). For comparison, a similar sample (CoPc thin film) was prepared by thermal evaporation at the same temperature (428 K), and the SEM of this sample is shown in Fig. 6(b). It is easily observed that the sample prepared by thermal evaporation contains a pore while that prepared by drop-casting contains stick structures with no pores at all.

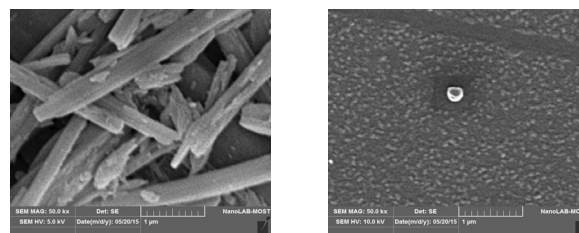


Fig. 6 SEM images of CoPc thin film samples prepared at the temperature of 428 K by (a) drop-casting and (b) thermal evaporation.

The absorbance of the CoPc thin film is shown in Fig. 7, where the spectrum has two bands, one is in the ultraviolet (UV) region, called B-band (or sort) at 330 nm, and the other is in the visible region (610 nm – 690 nm), called Q-band, and consists of two close peaks. We can see a flat area in the region of 380 nm – 530 nm.

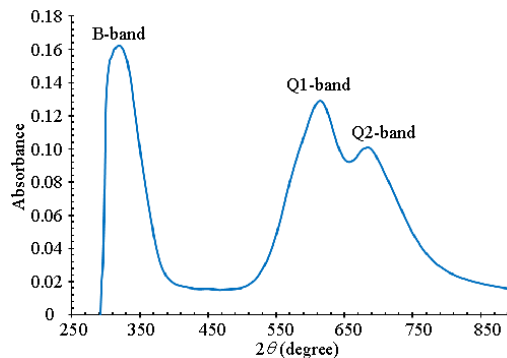


Fig. 7 Absorbance of the CoPc thin film as a function of the wavelength.

The optical energy gap (E_g) of CoPc thin films was determined by the Tauc equation used to find the type of optical transition by plotting $(ahv)^2$ versus photon energy (hv) as shown in Fig. 8. This shows that E_g equals 3.41 eV.

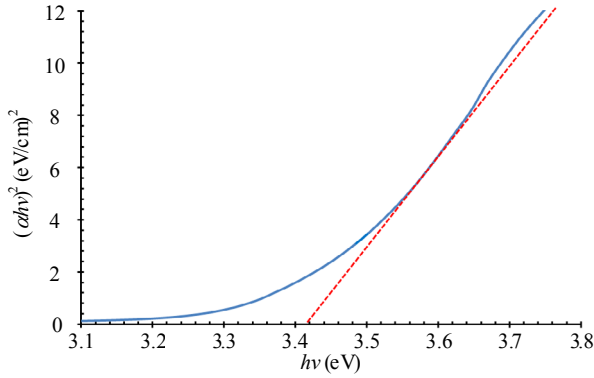


Fig. 8 Plot of $(ahv)^2$ versus photon energy (hv) of incident radiation for the CoPc thin film.

The changes in the capacitance depend upon the area of the plate, film thickness, and dielectric properties of the sensing materials. In general, the relationship between the relative dielectric constant and polarizability is determined by Clausius-Mosotti relation [19]:

$$\frac{(\varepsilon_{\text{dry}} - 1)}{(\varepsilon_{\text{dry}} + 1)} = \frac{N_{\text{ary}} \alpha_{\text{dry}}}{3\varepsilon^\circ} \quad (1)$$

where ε_{dry} is the relative permittivity, and ε° is the permittivity of free space. From the above equation, we can write the expression in %RH humidity:

$$\varepsilon_{\text{dry}} = \frac{(1 + 2N_{\text{ary}} \alpha_{\text{dry}} / 3\varepsilon^\circ)}{(1 - N_{\text{ary}} \alpha_{\text{dry}} / 3\varepsilon^\circ)} \quad (2)$$

A similar equation can be written for the dielectric constant at higher humidity:

$$\varepsilon_H = \frac{(1 + 2N_H \alpha_H / 3\varepsilon^\circ)}{(1 - N_H \alpha_H / 3\varepsilon^\circ)} \quad (3)$$

The value of $N_H \alpha_H$ depends upon the relative humidity level. Therefore, the product $N_H \alpha_H$ can be assumed as

$$N_H \alpha_H = N_H \alpha_H (1 + KH) \quad (4)$$

The equation of the dielectric constant and capacitance for humidity can be written as

$$\frac{C_H}{C_{\text{dry}}} = \left(\frac{\varepsilon_H}{\varepsilon_{\text{dry}}} \right)^n \quad (5)$$

From (2) to (5), the relationship between the capacitance and dielectric constant of the humidity sensor can be written as

$$\frac{C_H}{C_{\text{dry}}} = \left(\frac{(1 + 2N_{\text{dry}} \alpha_{\text{dry}} (1 + KH) / 3\varepsilon^\circ)}{(1 - N_{\text{dry}} \alpha_{\text{dry}} (1 + KH) / 3\varepsilon^\circ) \varepsilon_{\text{dry}}} \right)^n \quad (6)$$

where H is the relative humidity, and K is the humidity capacitive factor.

The measured capacitance-humidity relationships of Al/CoPc/Al surface-type humidity sensor are shown in Fig. 9. It is observed that the capacitance increases nonlinearly with increasing humidity level from 45%RH to 95%RH. It is seen that the capacitance of the sensor increases with an increase in frequency (12 Hz, 100 Hz, 300 Hz, and 600 Hz). As well, an increase in capacitance with increasing the relative humidity can be explained on the basis of the absorption of the water vapor in the pores of the active material (CoPc thin film). The dielectric constant of the active material is changed with the adsorption of water vapors due to the formation of charge-transfer complexes by H_2O , which consequently increases the capacitance.

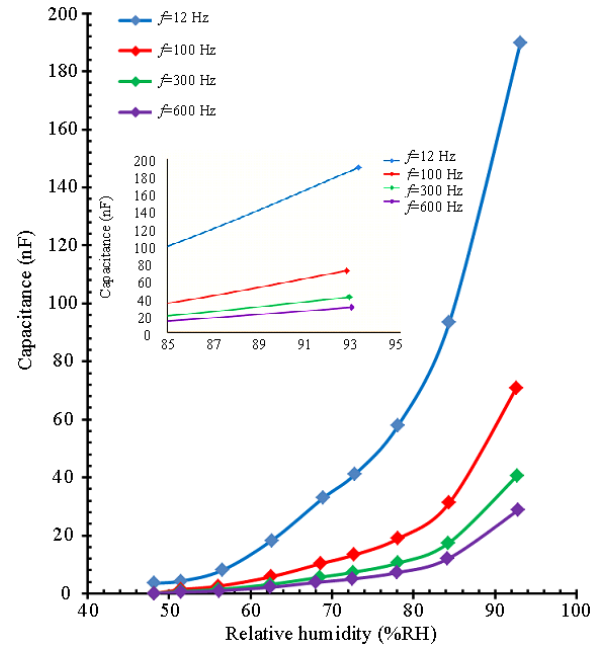


Fig. 9 Capacitance-relative humidity relationships of the Al/CoPc/Al humidity sensor.

Figure 10 shows the relationship between the resistance and relative humidity of the fabricated

Al/CoPc/Al surface-type humidity sensor. It is seen from this figure that the resistance of the humidity sensor decreases nonlinearly with increasing level of the relative humidity. The resistance values decrease from 6556 k Ω , 2850 k Ω , 2397 k Ω , 2218 k Ω to 64.3 k Ω , 23.66 k Ω , 14.43 k Ω , and 10.5 k Ω at frequencies of 12 Hz, 100 Hz, 300 Hz, and 600 Hz, respectively.

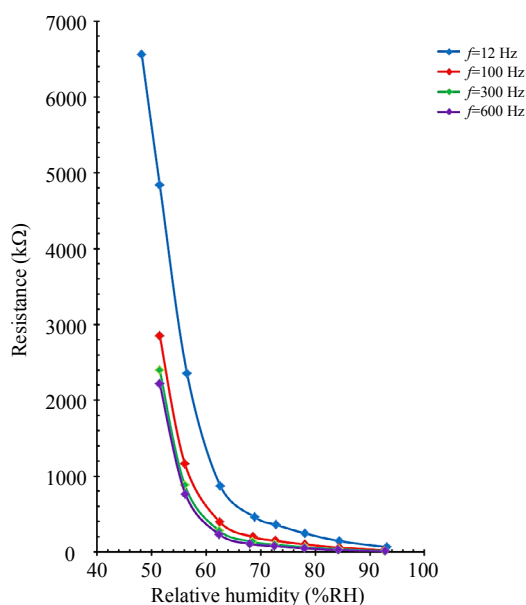


Fig. 10 Resistance-relative humidity relationships of the Al/CoPc/Al humidity sensor.

4. Conclusions

In this paper, the following main conclusions can be highlighted. A surface-type capacitive organic humidity sensor was fabricated from the Al/CoPc/Al structure by the drop-casting technique on glass substrates. The performance of this humidity sensor was experimentally studied. The X-ray diffraction patterns of CoPc thin films showed the single-crystalline β -phase tetragonal structure, which was preferentially oriented in (100) plane. The absorbance of the CoPc films showed two bands in the UV and visible regions. The capacitance of the fabricated sensor was increased while its resistance was decreased with increasing humidity level due to an increase in the concentration of H₂O molecules and hence the displacement current. The capacitive humidity sensors fabricated in this work showed a good

linearity and exhibited a better stability at higher humidity as compared with resistive humidity sensors.

Acknowledgement

Authors would like to thank Dr. Oday A. Hammadi at Al-Iraqia University for his valuable assistance in preparation and submission of this manuscript.

Open Access This article is distributed under the terms of the Creative Commons Attribution License which permits any use, distribution, and reproduction in any medium, provided the original author(s) and source are credited.

References

- [1] Q. Weng and S. Yang, "Urban air pollution patterns, land use, and thermal landscape: an examination of the linkage using GIS," *Environ Monit Assess*, 2006, 117(1-3): 463-489.
- [2] Y. Anjaneyulu, I. Jayakumar, V. H. Bindu, P. V. M. Rao, G. Sagaraswar, K. V. Ramani, *et al.*, "Real-time remote monitoring of air pollutants and their online transmission to the web using internet protocol," *Environ Monit Assess*, 2007, 124(1-3): 371-381.
- [3] A. Joyce, J. Adamson, B. Huntley, T. Parr, and R. Baxter, "Standardisation of temperature observed by automatic weather stations," *Environ Monit Assess*, 2001, 68(2): 127-136.
- [4] Z. M. Rittersma, "Recent achievements in miniaturised humidity sensors - a review of transduction techniques," *Sensors and Actuators A: Physical*, 2002, 96(2-3): 196-210.
- [5] C. Y. Lee and G. B. Lee, "Humidity sensors: a review," *Sensor Letters*, 2005, 3(1-4): 1-15.
- [6] Z. Chen and C. Lu, "Humidity sensors: a review of materials and mechanisms," *Sensor Letters*, 2005, 3(4): 274-259.
- [7] F. Aziz, M. Sayyad, K. S. Karimov, M. Saleem, Z. Ahmad, and S. M. Khan, "Characterization of vanadyl phthalocyanine based surface-type capacitive humidity sensors," *Journal of Semiconductors*, 2010, 31(11): 114002.
- [8] G. Liang, T. Cui, and K. Varahramyan, "Electrical characteristics of diodes fabricated with organic semiconductors," *Microelectronic Engineering*, 2003, 65(3): 279-284.
- [9] M. Irimia-Vladu, N. Marjanovic, M. Bodea, G. Hernandez-Sosad, A. M. Ramil, R. Schwödianer, *et al.*, "Small-molecule vacuum processed melamine - C₆₀, organic field-effect transistors," *Organic*

- Electronics*, 2009, 10(3): 408–415.
- [10] G. Garcia-Belmonte, P. P. Boix, J. Bisquert, M. Sessolo, and H. J. Bolink, “Simultaneous determination of carrierlifetime and electron density-of-states in P3HT: PCBM organic solar cells under illumination by impedance spectroscopy,” *Solar Energy Materials and Solar Cells*, 2010, 94(2): 366–375.
- [11] I. Ling and L. Chen, “Organic light-emitting diode performance enhancement via indium tin oxide glass surface modification,” *Current Applied Physics*, 2010, 10(1): 346–350.
- [12] I. Muzikante, V. Parra, R. Dobulans, E. Fonavs, J. Latvels, and M. Bouvet, “A novel gas sensor transducer based on phthalocyanine heterojunction devices,” *Sensors*, 2007, 7(11): 2984–2996.
- [13] P. J. Kivits, R. D. Bont, and J. V. D. Veen, “Vanadyl phthalocyanine: an organic material for optical data recording,” *Applied Physics A*, 1981, 26(2): 101–105.
- [14] A. N. Burgess, K. E. Evans, M. Mackay, and S. J. Abbott, “Comparison of transient thermal conduction in tellurium and organic dye based digital optical storage media,” *Journal of Applied Physics*, 1987, 61(1): 74–80.
- [15] B. Joseph and C. Menon, “Studies on the optical properties and surface morphology of cobalt phthalocyanine thin films,” *E-Journal of Chemistry*, 2008, 5(1): 86–92.
- [16] F. Gutman and L. Lyons, *Organic semiconductors*. Malabar, Florida: Krieger Publishing Company, 1981.
- [17] O. A. Hamadi, “Characteristics of CdO-Si heterostructure produced by plasma-induced bonding technique,” *Proc. IMechE PartL: J. Materials: Design and Applications*, 2008, 222, L1: 65–71.
- [18] O. A. Hammadi, “Photovoltaic properties of thermally-grown Se-doped silicon photodiodes for infrared detection applications,” *Photonic Sensors*, 2015, 5, 2: 152–158.
- [19] M. Shah, M. H. Sayyad, and K. S. Karimov, “Fabrication and study of nickel phthalocyanine based surface type capacitive sensors,” *World Academy of Science, Engineering and Technology*, 2008, 43: 392–394.